

Segmentation of forest patches and estimation of
canopy cover using 3D information from stereo
photogrammetry

Ann-Helen Granholm

Faculty of Forest Science

Department of Forest Resource Management

Umeå

Licentiate Thesis

Swedish University of Agricultural Sciences

Umeå 2016

Cover: Reference plot in a pasture with Oak trees (*Quercus robur* L.). Left: colour-infrared orthophoto with plot boundary. Right: image-based point cloud viewed from the side.

ISBN (print version) 978-91-576-9399-0

ISBN (electronic version) 978-91-576-9400-3

© 2016 Ann-Helen Granholm, Umeå

Print: SLU Service/Repro, Uppsala/Alnarp 2016

Segmentation of forest patches and estimation of canopy cover using 3D information from stereo photogrammetry

Abstract

3D information extracted by image matching of aerial images, so called image-based point clouds, have been found to provide accurate vegetation height measurements. This has led to an increased interest from the vegetation mapping community, since aerial images are an affordable alternative to airborne laser scanner (ALS) data. In Sweden, this is especially interesting due to the national mapping agency's decision to derive 3D information from annually acquired aerial imagery, starting in 2016. Previous studies have shown that image-based point cloud data derived from standard stereo aerial images is of potential use for forest inventory and change detection.

In this thesis, the focus is on exploring the utility of image-based point clouds, and surface models, for vegetation mapping; more specifically, it explores segmentation of vegetation patches based on height above ground, estimation of tree height, and estimation of vertical canopy cover. The studies were conducted in a study area located in the hemi-boreal zone of southern Sweden.

Segmentation based on canopy height models (CHMs) derived by image matching combined with a digital elevation model (DEM) from ALS data was found to deliver polygons within which tree height varied with a few meters. Tree height was estimated using height percentiles derived from the CHM and the results were similar to previous studies using image-based point clouds. Estimation of vertical canopy cover resulted in low accuracy due to underestimation when the canopy cover was sparse, and overestimation when the canopy cover was dense, while behaving linearly at approximately 15 – 85 % canopy cover. Dominant tree species influenced the results of estimation of tree height, as well as vertical canopy cover.

Vegetation mapping using image-based point cloud data holds great potential and further research is needed to gain knowledge of appropriate methods and limitations.

Keywords: stereo photogrammetry, aerial images, vegetation mapping, segmentation, vertical canopy cover

Author's address: Ann-Helen Granholm, SLU, Department of Forest Resource Management,
901 83 Umeå, Sweden
E-mail: ann-helen.granholm@slu.se

Dedication

Till Daniel, Alice och Kalle

Goda överblicksbilder tar man bäst från toppen av ett träd, ännu bättre från ett flygplan. Överblicken vinnes som alltid på bekostnad av detaljerna: de små strukturerna försvinner.

Hugo Sjörs, Myrvegetation i Bergslagen, 1948

Contents

List of Publications	7
Abbreviations	9
1 Introduction	11
1.1 Vegetation mapping in Sweden – a background	11
1.2 Photogrammetry	13
1.2.1 Stereo photogrammetry	13
1.2.2 Automatic extraction of 3D information from stereo aerial images	14
1.2.3 Factors influencing the quality of image-based point clouds	14
1.3 Using image-based point cloud data for mapping forest	16
1.3.1 Stereo overlap and height accuracy	16
1.3.2 Segmentation	18
1.3.3 Canopy cover	20
1.3.4 Multitemporal data	21
1.3.5 Using stereo aerial images for production of nationwide data	22
1.3.6 Outlook in Sweden	22
2 Objectives	24
3 Materials and methods	25
3.1 Materials	25
3.1.1 Study area	25
3.1.2 Remotely sensed data	27
3.1.3 Reference data	28
3.2 Methods	29
3.2.1 Processing of ALS data	29
3.2.2 Image matching	29
3.2.3 Canopy Height Models	30
3.2.4 Segmentation (paper I)	31
3.2.5 Evaluation of segmentation (paper I)	31
3.2.6 Evaluation of tree height (paper I)	31
3.2.7 Estimation of vertical canopy cover (paper II)	32
4 Results and general discussion	33
4.1 General results	33
4.2 Segmentation (paper I)	33

4.3	Tree height estimation (paper I)	37
4.4	Vertical canopy cover (paper II)	38
5	Conclusions	43
	References	45
	Acknowledgements	52

List of Publications

This thesis is based on the work contained in the following papers, referred to by Roman numerals in the text:

- I Granholm, A., Olsson, H., Nilsson, M., Allard, A., and Holmgren, J. (2015). The potential of digital surface models based on aerial photos for automated vegetation mapping. *International Journal of Remote Sensing* 36 (7), 1855 - 1870.

- II Granholm, A., Lindgren, N., Olofsson, K., Nyström, M., Allard, A. and Olsson, H. Estimating vertical canopy cover using dense image-based point cloud data in four vegetation types in southern Sweden. (Submitted)

Paper I is reproduced with the permission of the publishers.

The contribution of Ann-Helen Granholm to the papers included in this thesis was as follows:

- I Planned the field inventory in co-operation with the supervisors. Carried out the aerial photo interpretation as well as image analysis and segmentation. Performed the statistical analysis with the help of colleagues knowledgeable in the programming language R. Wrote the major part of the paper.
- II Planning in cooperation with co-authors. Performed the aerial photo interpretation, matching of images, and the statistical analysis. Wrote the majority of the manuscript.

Abbreviations

ALS	Airborne Laser Scanning
CHM	Canopy Height Model
CIR	Colour Infrared
DEM	Digital Elevation Model
DMC	Digital Mapping Camera by Zeiss/Intergraph
DSM	Digital Surface Model
DTM	Digital Terrain Model, same as DEM
GIS	Geographical Information System
LiDAR	Light Detection and Ranging
nDSM	Normalized Digital Surface Model, same as CHM
NILS	National Inventory of Landscapes in Sweden
UAV	Unmanned Aerial Vehicle
VCC	Vertical Canopy Cover
VR	Vegetation Ratio

1 Introduction

Monitoring and management of natural resources requires regularly updated and accurate geographical information. With the variety of landscape types such as forest, wetland, arable land, impediments due to climate or soil properties, and built up areas, it is a challenge to produce geographical information which fills all needs. Remote sensing techniques are commonly applied to generate large area maps or raster data, automatically and with high spatial accuracy (Lillesand, Kiefer and Chipman 2008). Such data should be sufficiently detailed, both in spatial resolution and in the number of classes, and the methods used should be time and cost-efficient. One essential task is the separation of non-forest areas from forest, for example, according to FAO's definition (2010) which is based on criteria such as minimum tree cover, potential vegetation height and land use.

1.1 Vegetation mapping in Sweden – a background

Visual interpretation of color infrared (CIR) aerial images has been used in several mapping projects in Sweden. The currently available vegetation maps in Sweden, covering approximately 47 % of the country including the mountainous area were derived by visual stereo interpretation of CIR aerial imagery during the years 1975 to 2009 (Andersson 2010, Ihse 2007). The lack of updated vegetation data is of concern for nature conservation and research, as well as for recreational activities and tourism. The Swedish National Wetland Inventory (VMI) was a national vegetation mapping project focused on inventory and mapping of wetlands by using a combination of visual stereo interpretation of aerial imagery and field inventories (Gunnarsson and Löfroth 2009), and was performed in a number of counties in Sweden. In Natura2000, habitats in protected areas in Europe were mapped, and in Sweden this was

done by visual interpretation of aerial images combined with field visits (Naturvårdsverket 2009).

The National Inventory of Landscapes in Sweden (NILS) programme aims to monitor the condition and changes in the Swedish landscape to provide statistics as well as data for studies of biodiversity, landscape development and cultural heritage (Ståhl et al. 2011). This is accomplished through data collection using a repeated field inventory of 631 permanent squares distributed over the whole of Sweden, as well as by wall-to-wall mapping of $1 \times 1 \text{ km}^2$ around each area by visual stereo interpretation in aerial images where vegetation types are delineated by polygons, based on clearly visible borders in the landscape as well as on predetermined threshold values of different vegetation characteristics (Allard et al. 2003). The data gathered by NILS has been used in several studies regarding biodiversity (e.g., Gao et al. 2014, Hedblom and Söderström 2011, Jeglum et al. 2011, Ottvall et al. 2008, Ortega et al. 2011). Lindgren et al. (2015) found that wall-to-wall mapping of $5 \times 5 \text{ km}^2$ areas around each of the 631 permanent areas in NILS could be done based on classification of a combination of vegetation height and canopy cover from ALS data, spectral information from optical satellite data, as well as field inventory data and visual interpretation. THUF, Terrestrial Habitat Monitoring, is a project aiming to gather information on valuable habitats outside of protected sites, which uses visual interpretation of aerial images and field inventory (Gardfjell and Hagner 2011).

Optical satellite data can cover large areas per scene, and have been used in several projects for producing national coverage of data on forest, such as the SLU Forest Map (SLU 2015), which is a national database with estimates of forest variables such as tree height, age, and wood volume for the years 2000, 2005, and 2010 (SLU 2015, Reese et al. 2003). Another example is the Swedish contribution to the CORINE Land Cover database, representing the land cover in the year 2000 based on optical satellite data (Hagner and Reese 2007, Naturvårdsverket 2014). Satellite-based change detection in wetlands was performed in several counties in Sweden, based on the method described in Boresjö-Bronge and Näslund (2002). A combination of satellite data and visual interpretation of aerial images was used to map nature reserve areas in Sweden (Naturvårdsverket 2004). CadasterENV is a currently running project, aiming to develop methods for national land cover mapping using a combination of optical satellite data from different sensors and airborne laser scanner data, and recently the Swedish Environmental Protection Agency decided to initiate a national land cover mapping project. Nordkvist et al. (2012) found that combining optical satellite data and ALS data increased the accuracy for different tree species classes as compared to using solely satellite

data. The classification accuracy of mountain birch (*Betula pubescens ssp. czerepanovii*) and alpine willow (*Salix spp.*) has also been found to increase by the combined use of optical satellite data and ALS data (Reese et al. 2014).

A raster database with estimates of forest variables that covers all of Sweden has been produced using a combination of field data from the Swedish National Forest Inventory (NFI) and ALS data acquired by Lantmäteriet for the production of the new national elevation model (Nilsson, submitted). All raster estimates are available free of charge from the Forest Agency's homepage (Skogsstyrelsen 2015).

In this thesis, the focus is on vegetation mapping using 3D information extracted from stereo aerial images by image matching, and more specifically delineation of vegetation based on their height above ground, and estimating vertical canopy cover.

1.2 Photogrammetry

1.2.1 Stereo photogrammetry

Photogrammetry is the science and technology of obtaining spatial measurements from photographs (Lillesand, Kiefer and Chipman 2008). Visual stereo interpretation utilizes the depth perception created by the human brain when observing stereo overlapping images. For instance, a stereogram is created using two overlapping images arranged side by side with a displacement approximately the same as the distance between the eyes of a human (Boberg 2001). With analogue images, analytical stereo plotters were used to enable stereo photogrammetric measurement. This is the registering of image coordinates of objects in the images using the depth perception of an interpreter. The image coordinates could be used to recreate the rays of light from the objects on the ground to the center of the projection, thus rendering 3D coordinates in a geodetic coordinate system. This is enabled by knowledge of the inner orientation of the camera through camera calibration, meaning the location of the focal point, the focal length, image coordinate system, and lens distortion. Aerial stereo photogrammetry, developed in the early 20th century, has experienced a revival during the last decades due to the development of digital cameras alongside the development of digital photogrammetric work stations and the increase in computer capacity concerning memory and processors (Baltsavias 1999, Leberl 2010). Digital cameras have sensors constructed either as a matrix of charge coupled device (CCD) arrays, or as line scanners with single, or multiple, CCD arrays. Images acquired using matrix CCD cameras are in focus in this thesis.

1.2.2 Automatic extraction of 3D information from stereo aerial images

Going from analogue to digital cameras meant improved dynamic range and improved signal-to-noise ratio of the aerial images, which allowed for a great number of homologous points to be extracted through image matching (Haala 2009), as did the increase in stereo overlap (Hirschmugl 2008). Today, there is a multitude of software solutions for the production of dense 3D point cloud data derived by stereo photogrammetry, so-called image-based point clouds (Haala 2014, Hirschmüller 2008, Middlebury Stereo Benchmark 2016, Remondino et al. 2014).

In this thesis, the commercially available photogrammetric software MATCH-T DSM by Inpho/Trimble (Lemaire 2008, Heuchel et al. 2011), and SURE by nFrames (Rothermel et al. 2012) were used to produce image-based point clouds, or surface models. The input data were aerial images with interior and exterior orientation, and camera information such as focal length, image coordinate system, lens distortions acquired by camera calibration, and flight altitude.

1.2.3 Factors influencing the quality of image-based point clouds

The accuracy and density of the output of image matching depends on several factors, some of them are (Haala 2009, Honkavaara et al. 2012, McGlone and Lee 2013):

- the image quality, sufficient stereo overlap and spatial resolution,
- quality of the camera model,
- the suitability of the stereo matching algorithm to the object of interest, and
- the geometric complexity of the object of interest.

Forest is an object type which is generally conceived of as difficult for image matching (Anon 2014a, Haala 2009, Ginzler and Hobi 2015). Matching will only produce points representing objects which are detectable in overlapping images, which is why, for instance, point cloud data over a dense forest canopy represents the upper surface of the canopy (Baltsavias 1999).

Image matching is limited by the difference in perspective projections, which will increase with the angle between the viewing directions and with the roughness of the recorded surface. Sometimes the difference in perspective will lead to occlusion (McGlone and Lee 2013). Occlusion means that an object is not visible in the image since another object is blocking the view from the camera. In the case of imagery acquired using a matrix CCD-camera, as in this thesis, occlusion is more likely to occur closer to the edges of the image due to bi-directional displacement, i.e., objects appear to lean away from the centre of

the image. Occlusion is a common problem with image matching in forest areas, due to trees being behind or in-between other trees, especially if the tree crowns are long (Haala 2009, St Onge et al. 2015). For instance, the far side of a forest edge in relation to the camera position will not be visible in the images and will therefore not be represented in the image-based point cloud. In close-range stereo photogrammetry, this is solved by acquiring stereo coverage from many angles around the object of interest. A similar approach in aerial image acquisition would acquire higher stereo overlap both along-track and across-track.

The reflectance of the surface might differ in different perspectives, rendering it difficult to find a match (St Onge et al. 2008, McGlone and Lee 2013). The accuracy of the image-based point clouds is sensitive to shadows (Haala 2014, Honkavaara et al. 2012), partly since objects in the shadow are more difficult to match due to the lack of spectral information, but also because of shadow movement. The amount of shadow in the images can be reduced by limiting image acquisition to hours with high sun elevation, which reduces the length of shadows. The effect of moving shadows on matching results can be reduced by restricting matching to images from within the same strip (Anon 2014a).

Images with good contrast yield better matching results when using area-based and feature-based matching algorithms (McGlone and Lee 2013). Algorithms using correlation windows (template and search windows) result in smoothing effects, for instance, at object borders and height discontinuities (Haala and Rothermel 2012, Klang 2015, St Onge et al. 2008). Repetitive patterns might result in erroneous matching (McGlone and Lee 2013).

Technical advances have also enabled three-dimensional (3D) stereo vector digitizing, for instance, by using GIS interfaces and 3D stereo vector superimposition. This has facilitated efficient visual stereo interpretation of vegetation in aerial images.

Today, it is possible to mount consumer-size digital cameras on unmanned aerial vehicles (UAVs) to acquire very high resolution aerial imagery with high stereo overlap at a low cost. Apart from aerial cameras pointed downwards, acquiring nadir aerial images, it is possible to mount aerial cameras slightly tilted to the side, thereby acquiring oblique images. In this thesis, the focus is on using digital aerial photographs acquired with nadir-pointing aerial mapping cameras mounted on manned airplanes.

1.3 Using image-based point cloud data for mapping forest

Several studies have demonstrated the accuracy in horizontal coordinates and the height of the extracted 3D information, as well as the high point density of image-based point clouds derived from aerial stereo images (Cramer and Haala 2010, Haala 2014). Since the image-based point clouds hold little or no information about ground elevation in areas with tree cover, an accurate DEM is needed for normalizing the image-based point cloud to height above ground (Baltsavias 1999).

In forestry, image-based point clouds, or surface models derived from these, have shown potential for estimation of forest variables such as tree height, basal area and stem volume at the stand level (Bohlin et al. 2012, Järnstedt et al. 2012, Nurminen et al. 2013, Vastaranta et al. 2013, White et al. 2013, Straub et al. 2013, Pitt et al. 2014, Gobakken et al. 2015, Stepper et al. 2015a). Studies of individual tree detection and classification using image-based point clouds, or surface models, have also shown promise (Hirschmugl 2008, Wallerman et al. 2012, St Onge et al. 2015, Rahlf et al. 2015).

1.3.1 Stereo overlap and height accuracy

Image acquisition with an along-track stereo overlap of 60 % and across-track overlap of 30 % was cost efficient when using analogue aerial cameras. This setup is still common, though digital cameras are capable of acquiring images with an 80 % along-track overlap without changing the flight altitude or flight speed (Leberl et al. 2010). When matching images covering forest, using images with a 60 % along-track stereo overlap might lead to mismatches causing inaccurate measurements, or no matches leading to low point densities, due to the difference in perspective (Hirschmugl 2008, Lemaire 2008). Using an 80 % stereo overlap results in denser point clouds and may reach down to the terrain surface in canopy gaps, thus yielding cognitively better results compared to 60 % (Nurminen et al. 2013, St Onge et al. 2015). Thus larger along-track stereo overlap is generally preferred (Hirschmugl 2008, Nurminen et al. 2013, Honkavaara et al. 2013, Anon 2014a, Anon 2014b).

The height accuracy of stereo measurements is however dependent on the base-to-height ratio, the base being the distance between camera positions when acquiring the images, meaning that aerial images with a large stereo overlap has a smaller base-to-height ratio which leads to lower height accuracy (Boberg 2001). For instance, Honkavaara et al. (2012) compared the height of signalized ground control points to DSMs derived by image matching of individual stereo models with 60 % stereo overlap, and 80 %, respectively, and found that the root mean square error (RMSE) of height was $0.5 - 2 \times$ the ground sampling distance (GSD). The increase in stereo overlap, from 60 % to

80 %, caused a 1.3 – 2.3 fold increase in the random height error (Honkavaara et al. 2012). This is likely not the case in practical application, when multi-image matching is preformed (Honkavaara et al. 2012). An example is the results by Hirschmugl (2008) who compared canopy height models (CHMs) derived from image-based point clouds to field measured individual tree height, and found that using a matching strategy which included image pairs with stereo overlap of approximately 90 % along-track resulted in a mean height error of 0.8 m and standard deviation (SD) of 2.4 m, while using a CHM derived from images with a stereo overlap of 60 % resulted in an mean height error of 1.3 m and SD of 4.5 m. This increase in accuracy despite low base-to-height ratio was accredited to the matching method which collected several corresponding matching results which yielded a comparable wide-spread bundle of multiple projection lines, thereby assuring numeric and geometric stability for the determination of ground coordinates (Hirschmugl 2008). A factor which contributed to the mean height error in the image-based point clouds was the general offset, which was thought to be caused by an inner image distortion found in the UltraCam (Honkavaara et al. 2006). However, the accuracies obtained were in line with the expected accuracy of field measurement (Hirschmugl 2008).

Using image-based point clouds as data for estimation of forest variables is interesting due to the availability of data at a relatively low cost in comparison to ALS data. Aerial imagery with a standard stereo overlap, generally a stereo overlap of 60 % along-track and 20 – 30 % across-track (Leberl et al. 2010, Boberg 2001), can be acquired at a higher flight altitude and at a higher speed compared to ALS data acquisition (Leberl et al. 2010). So far, studies have shown that aerial images acquired with the standard stereo overlap of 60 % along-track, provide data for stand-level estimations of forest variables with accuracies comparable to ALS data. Increasing the stereo overlap, for instance to 80 % along-track overlap, yields only slightly more accurate results (Bohlin et al. 2012, Nurminen et al. 2013). A possible explanation for these results is that the image-based point clouds derived from aerial images with a stereo overlap of 60 % along-track were sufficiently dense for stand level estimation of forest variables, in which the heights are summarized and averaged over an area. When it comes to ALS point clouds, it has been found that an increase in point density has little effect on plot level estimation in case the height distribution of points within the plot is unchanged (Lim et al. 2008).

A CHM derived by area-based matching methods is generally smoother than a CHM derived from ALS data (e.g. St Onge et al. 2008). Large window sizes in area-based matching allows for a wider search for homologous points, compared to using small windows, but they also increase the smoothing effect

(St Onge et al 2008). Comparison of CHMs derived by image matching applied to scanned aerial images and normalized using a DEM from ALS data to CHMs based on ALS data showed that they were highly correlated ($r = 0.89$), but the image-based CHMs had a lower spatial resolution and accuracy (St Onge et al. 2008).

Solar elevation can also have an effect on the height accuracy of image-based point clouds. St Onge et al. (2008) found that left-right differences in the images making up stereo models (e.g. the sunlit side of a tree canopy is visible in one image and the shadowed side of the same trees is visible in the second image), resulted in less accurate height in the CHMs derived from image matching. Honkavaara et al. (2012) found that solar elevation had no effect on image matching results in sunlit and flat areas, while the random height variation increased up to 3 times for flat shadowed areas. Differences were larger in the forest, where a systematic difference indicated that image matching was able to find homologous points between the trees when the sun elevation was higher, while only points in the upper canopy surface were found when the sun elevation was low (Honkavaara et al. 2012). The random differences in the DSMs covering forest were about 1 – 3 m and possible explanations are vagueness of measured points, uncertainty in image matching due to large disparities in the windows and large height variations in the forest (Honkavaara et al. 2012). Similar results in forested areas were reported in Baltasvias et al. (2008) and St Onge et al. (2008).

1.3.2 Segmentation

With high resolution data such as a CHM with pixel size of 0.5 m, pixel-based processing might not be advisable since the pixel might not represent the object of interest (Hirschmugl 2008) or the same object might be represented by several pixels with differing properties such as spectral information or height. One approach is to use segmentation to derive objects rather than pixels (Pekkarinen 2002, Blaschke 2010, Leckie 2003).

Delineation based on visual interpretation of stereo aerial CIR imagery is a common method which produces high quality results thanks to the human capacity to recognize objects in a more flexible way than automatic methods, for instance to detect trees, estimate cover and classify species (Ihse 2007, Allard et al. 2003). The drawback of visual interpretation is the cost in time, as well as the difference between interpreters which might introduce error (e.g. Heiskanen et al. 2008).

Previous studies have shown that combining spectral information in images and 3D information such as vegetation height, yield high accuracy in segmentation and classification results (Matikainen and Karila 2011, Hellesten

and Matikainen 2013, Rapinel et al. 2015). Segmentation using only 2D information, such as an orthophoto, suffers from the trouble of separating spectrally similar objects such as shrubs and small trees from ground cover (Hellesen and Matikainen 2013) as well as differences in illumination and view angle. To apply segmentation to a surface model derived by image matching, such as a CHM, would have the benefit of delivering segments less influenced by view angle and illumination, as well as the vegetation height above ground. However, view angle and illumination influences image matching results, which may have an effect on the CHM and thus segmentation as well. For instance, St Onge et al. (2015) found that view angles above 16° resulted in lower point densities in image-based point clouds, compared to point density at near-vertical view angles. Large view angles caused an overrepresentation of heights in the upper canopy and underrepresentation of lower heights, primarily in dense coniferous stands, and less in open coniferous stands or deciduous stands (St Onge et al. 2015). Contradicting results were presented by Honkavaara et al. (2012), where the height error was found not to be dependent on the radial distance, i.e. distance to the center of the stereo model.

Prior to segmentation, a workflow of processing steps needs to be carried out to extract forest parameter information at an object-based level, such as geometric correction, topographic correction, radiometric correction, image fusion (pansharpening), and image enhancement (Hirschmugl 2008). Every step needs to be done with consideration to the subject of interest.

Regarding the surface structure of the CHMs, which is of importance for segmentation of tree crowns, a comparison of the CHMs in Hirschmugl (2008) showed that the CHM derived using a stereo overlap of approximately 90 % was nearly as detailed as the CHM based on ALS, with visible tree crowns and canopy gaps, while these details were not detectable in the CHM derived from images with 60 % stereo overlap.

Rahlf et al. (2015) found that segments of individual trees, derived by using a water-shed algorithm and a 0.5 m CHM from image-based point cloud data (15.6 points m⁻²), varied in size and there were errors due to omission errors in the image-based point cloud, such as trees in open areas that weren't visible in the point cloud.

In this thesis, segmentation was tested using eCognition 3.0 (Definiens Imaging GmbH, Munich, Germany), which uses a region-merging technique, starting with one-pixel objects which are merged step-wise with adjacent objects most similar to it, with regard to spatial and spectral properties (Baatz and Schäpe 2000).

1.3.3 Canopy cover

Vertical canopy cover is defined as the proportion of the area covered by the vertical projection of tree crowns (Jennings et al. 1999). Comparing CHMs from image-based point cloud data to CHMs derived from ALS data, it is clear that the latter are more detailed in the sense that small canopy gaps are mapped and tree crowns are visible (Hirschmugl 2008, Vastaranta et al. 2013), unless the images used to derive the image-based CHMs have a large stereo overlap and high spatial resolution in which case individual trees are visible in the CHMs (Hirschmugl 2008).

The lack of canopy gaps as well as no data areas due to omission, occlusion or deep shadow is generally the problem with deriving density metrics using image-based point clouds, or surface models derived from these (Vastaranta et al. 2013, St Onge et al. 2008, St Onge et al. 2015). Using canopy density metrics calculated as proportion of heights above a threshold (e.g. vegetation ratio) or as proportion of heights above height percentiles (e.g. CCmean which is the proportion of heights above mean height) were found to improve estimation accuracy for forest variable estimation in hemi-boreal broad-leaved forest and mixed forest (Stepper et al. 2015a, Straub et al. 2013), but not in complex boreal coniferous forest (White et al. 2015) or managed boreal coniferous forest (Vastaranta et al. 2013). White et al (2015) found that the similarity of metrics derived from ALS data and image-based point cloud data, respectively, increased with increasing canopy cover, especially metrics which describe the upper canopy. The observed differences between the above mentioned studies might be explained by a combination of both the difference in height distribution between ALS point clouds and image-based point clouds (Baltsavias 1999), and the difference in dominant tree species, which influences the shape and structure of the forest canopy. St Onge et al. (2015) found that coniferous trees with long tree crowns generally result in omission due to occlusion, while the effect of inter-tree occlusion was observed to a lesser degree in mixed species forest stands. Results such as these are reasons to encourage the development of metrics which are tailored to image-based point cloud data, e.g. Nurminen et al. (2013) who suggested some measure of proportion of crown area. The effect of tree species (e.g. Straub et al. 2013) could be mitigated by classification using the spectral information in the images. The color information of the image-based point cloud, extracted from the spectral bands of the matched aerial images during image matching, improved estimation accuracies of forest variables in a recent study (Rahlf et al. 2015), therefore there is reason to look into radiometric correction which might contribute to higher estimation accuracy (Korpela et al. 2011).

1.3.4 Multitemporal data

The regular update of aerial images enables change detection (Baltsavias et al. 2008) and studies of time series, including data assimilation. Nyström et al. (2015) took advantage of having aerial images from several years covering the same area in Sweden, and used CHMs derived from image-based point clouds representing different years as input to data assimilation which resulted in improved accuracy of forest variable estimation.

Waser et al. (2008) detected changes in shrub and tree cover in mire in Switzerland, by using DSMs derived by image matching. Wang et al. (2015) detected changes in forest in two study areas in Switzerland by comparing two DSMs generated by image matching of aerial images acquired three years apart, which resulted in high overall accuracy. The observed omission and commission errors could have been caused by the difference in sun elevation resulting in shadows in one year and no shadows in the other year. This could be resolved by shadow detection through spectral analysis and exclude these from the analysis. Another potential reason for errors is the difference in view angles of the imagery, causing an oblique problem between the DSMs. Any displacement, or offset, between the DSMs would also cause differences in DSMs (Wang et al. 2015).

Another change detection study aimed at detecting and classifying storm damage areas in coniferous and mixed forest in Finland by using DSMs derived by image matching (Honkavaara et al. 2013) resulted in successful detection of storm damage with high accuracy; results were 100 % correct in no damage areas, and 100 % correct in areas with more than ten fallen trees per ha. The method was insensitive to small damages, but this was considered as a minor problem (Honkavaara et al. 2013).

Stepper et al. (2015b) calculated annual growth in a German mixed forest as the change in forest height between two CHMs, derived by image matching of aerial image sets acquired five years apart. The overall annual growth based on CHMs from image matching was 0.30 m (SD: 0.53 m) and the corresponding measure derived from field measurements was 0.22 m (SD: 0.32 m) (Stepper et al. 2015b).

Vastaranta et al. (2016) classified forest stands by age using a time-series of eight CHMs derived from aerial images acquired between the years 1944 to 2012, resulting in an overall accuracy of 78.9 % when using changes in maximum height. Forest stands renewed after 1991 were correctly classified while older stands were classified with low accuracy, which might be caused by the lower quality of old archived images, but also due to uncertainty in reference age derived by counting rings in bore samples.

1.3.5 Using stereo aerial images for production of nationwide data

Ginzler and Hobi (2015) derived national coverage of DSMs for Switzerland through image matching of aerial images, acquired using a line scanner camera. During this work they found that the forest area was the most difficult to model, with RMSE of tree height varying from 3.4 – 5.5 m, with outliers excluded. The error increased with the distance to nadir, as well as with increasing slope inclination (Ginzler and Hobi 2015). CHMs were generated by normalizing the DSMs using a DEM based on ALS, and comparison of CHM to field measured single tree heights resulted in high correlation (Pearson's $r = 0.83$). However, lowland trees yielded higher correlation than trees at higher elevations, which could be explained by the lower resolution of the images at higher elevation (GSD of 0.5 m, compared to 0.25 m in the lowlands; Ginzler and Hobi 2015). The plot level canopy height also agreed well with the CHM, but here the coniferous tree dominated stands yielded higher correlation than the mixed tree stands (Ginzler and Hobi 2015). It was concluded that the CHM was likely most useful for stand-wise assessment, since the resolution of the images was too low to allow for individual tree estimation (Ginzler and Hobi 2015).

Waser et al (2015) used the DSMs generated by Ginzler and Hobi (2015) to generate a wall-to-wall forest map for Switzerland, which resulted in good overall accuracy of forest and non-forest. Classification was least accurate along forest edges and in areas with fragmented forest cover, especially in the treeline zone where the dominant coniferous tree species grow small and thus are difficult to extract for image matching (Waser et al. 2015).

Reese et al. (2015) performed classification of mountainous vegetation using a combination of optical satellite data and metrics derived by image matching in a limited area in the Swedish mountains. The results showed that classification of mountain birch (*Betula pubescens ssp. czerepanovii*) was slightly more accurate compared to classification using a combination of optical satellite data and metrics derived from ALS data (Reese et al. 2015), meaning that image-based point cloud data might be useful for mountain birch mapping in the mountainous region of Sweden.

1.3.6 Outlook in Sweden

The potential of using image-based point clouds for generation of maps or raster information is of great interest in Sweden, since Lantmäteriet, the National Land Survey of Sweden, has decided to generate image-based point clouds from the yearly acquisition of standard aerial stereo imagery. This makes up a national coverage of stereo aerial images, which is updated with an interval of two to ten years depending on the region. Due to the lack of

information about ground height beneath dense vegetation such as tree canopy in image-based point clouds, detailed elevation data such as a DEM derived from ALS ground returns are required to normalize the image-based point cloud, or surface model, to represent vegetation height. A new national digital elevation model (DEM) was recently produced by Lantmäteriet using ground returns in airborne laser scanning (ALS) data. There are a number of countries which have a similar situation with regards to data availability (Waser et al. 2015, White et al 2015). As expected, there are some limitations to image-based point clouds related to sensor (Baltsavias 1999) as well as the setup of image acquisition (St Onge et al. 2015, Vastaranta et al. 2013, White et al. 2015). The characteristics and utility of image-based point clouds need to be further investigated to fully understand the limitations as well as potential uses of image-based point cloud data for vegetation mapping.

2 Objectives

The general objective of the studies underlying this thesis was to investigate the usability of image-based point clouds and surface models for quantification and segmentation of vegetation in the Swedish landscape. The specific objectives were:

Paper I

- To evaluate the utility of normalized digital surface models generated by image matching of aerial imagery for automatic segmentation of vegetation patches, as well as for tree height measures in a managed hemi-boreal forest landscape.
- To compare the results of segmentation and tree height estimation using surface models derived from aerial imagery with high and low stereo overlap, as well as high and low spatial resolution.

Paper II

- To estimate vertical canopy cover using metrics calculated from image-based point clouds and surface models.

3 Materials and methods

3.1 Materials

3.1.1 Study area

The studies were conducted at the forest estate of Remningstorp, in the south of Sweden at Lat. 58° 30' N, Long. 13° 40' E (Figure 1). In Paper I a rectangular area of approximately 1.0 km by 1.5 km within the Remningstorp estate was used as study area. The main land cover was managed, hemi-boreal forest dominated by Norway spruce (*Picea abies* (L.) Karst.), Scots pine (*Pinus sylvestris* L.) and birch (*Betula* spp.). Within the test area there was also pasture, water and fragments of wetland.

Paper II had a study area of approximately 5 km by 8 km covering the Remningstorp estate and two nearby nature reserve areas: Eahagen and Klyftamon. The study was carried out within four vegetation types, which were treated as separate strata; 1) “Unmanaged forest” dominated by Scots pine in a nature reserve area, 2) “Deciduous” which was open and wooded pasture with a mix of hardwood broad-leaved trees Oak (*Quercus robur* L.) and Lime (*Tilia cordata* L.), other deciduous tree species such as Birch and Alder (*Alnus glutinosa* (L.) Gaertner), and occasionally Norway Spruce trees, 3) “Wetland” which was mainly open and wooded wetland in a nature reserve area dominated by Scots Pine on bog, and 4) “Managed“ forest of Scots Pine, Norway Spruce, and Birch on fertile sites. See Figure 1 for distribution of reference plots in the study area.

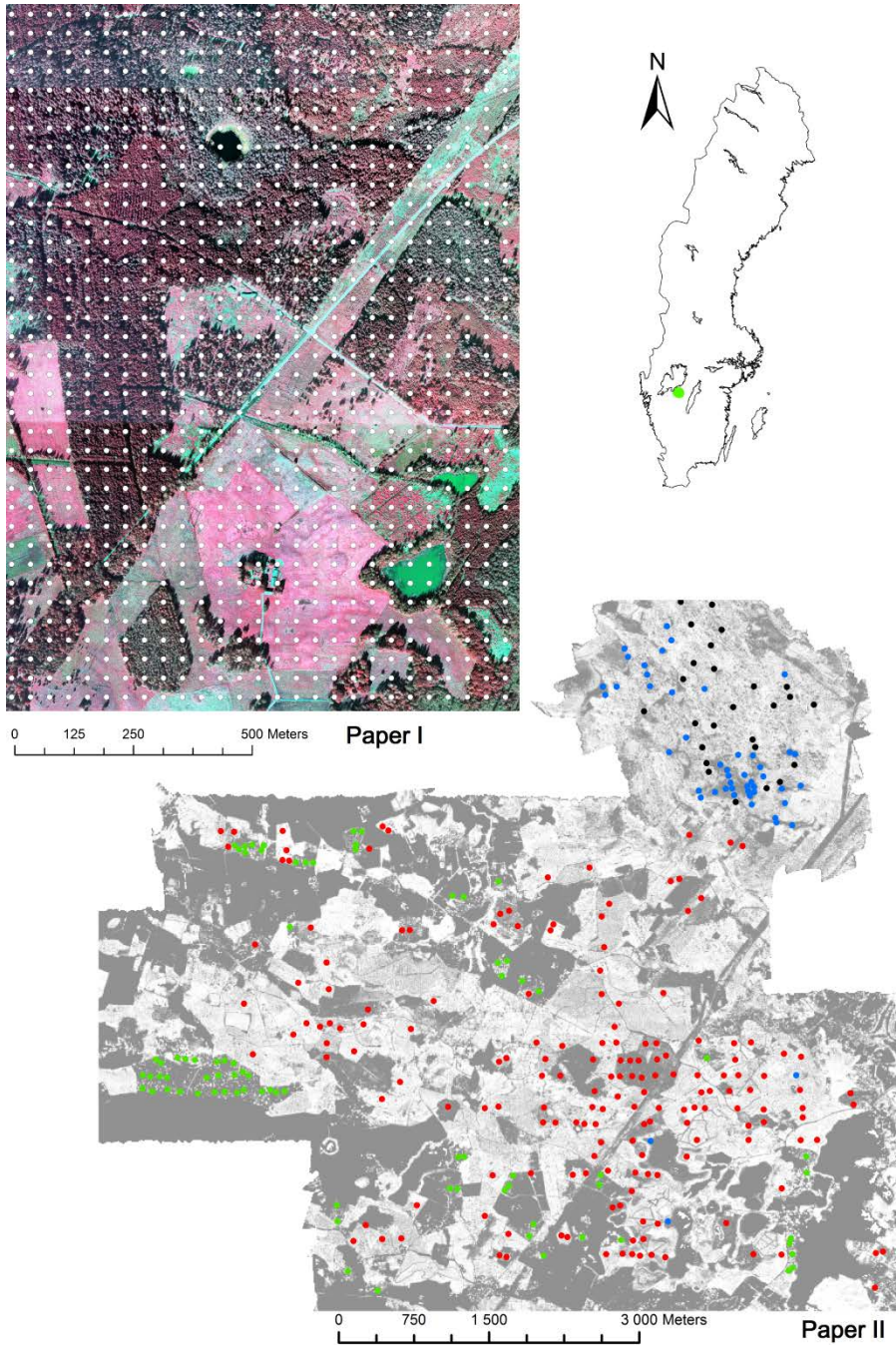


Figure 1. The location of the study area in southern Sweden. The area used in Paper I is illustrated by a CIR orthophoto with sample plots in white. The area used in Paper II is covered

by a canopy height model derived from ALS data with reference plots coloured by stratum; black = Unmanaged forest, blue = Wetland, green = Deciduous, red = Managed forest.

3.1.2 Remotely sensed data

The aerial images were acquired by Lantmäteriet. Images used in Paper I were acquired with the Digital Mapping Camera (DMC) by Zeiss/Intergraph, GmbH, which was operated between the years 2005 and 2013. Images used in Paper II were acquired with UltraCam Xpwa by Trimble, operated by Lantmäteriet from 2014. Lantmäteriet also operates an UltraCam Eagle by Trimble, from the year 2013 and onwards, but images acquired with this camera have not been used in this thesis. See specifications per aerial camera in Table 1, and information regarding image acquisition in Table 2. The ALS data used in this thesis are described in Table 3.

Table 1. Specifications for aerial cameras.

Camera	Z/I DMC	UltraCam Xpwa
Dynamic range (bit)	8 (12)	8 (16)
Bands	Pan, R,G,B, NIR	Pan, R, G, B, NIR
Pixel size (μm)	12	6
Number of camera heads	8 (4 panchromatic, 4 multispectral)	8 (4 panchromatic, 4 multispectral)
Focal length (mm)	120	70.5

Table 2. Acquisition details for aerial images. ¹ = Paper I, ² = Paper II.

Sensor	Z/I DMC ¹	Z/I DMC ¹	UltraCam Xpwa ²
Date	2009-09-01	2009-09-01	2014-07-26
Flight altitude a.g.l. (m)	1200	4800	2800
Stereo overlap (along-track/across-track)	80/60 %	80/30 %	60/27 %
GSD (m)	0.12	0.48	0.24
Bands	Pan-sharpened CIR, R, G, B	Pan-sharpened CIR, R, G, B	Pan-sharpened CIR, R, G, B

Table 3. Acquisition of ALS data. ¹ = Paper I, ² = Paper II.

Sensor	TopEye MkII ¹	Riegl LMS Q680 ²
Date	2008-09-04	2014-09-01
Flight altitude a.g.l.(m)	500	440
Pulse density (p m^{-2})	26	32 (within reference plots)

3.1.3 Reference data

In Paper I, reference data were obtained by visual stereo interpretation of mean tree height, proportion of diffuse vertical canopy cover (VCC; Jennings et al. 1999), and proportion of tree species in 993 sample plots using the CIR aerial images acquired at 1200 m above ground level (a.g.l.). The sample plots were circular with a radius of 10 m and were distributed in a regular grid with 40 m distance between plot centres (Figure 1). The reference data covered both open area and areas with dense tree cover (Figure 2). Of the 993 sample plots, 716 had vegetation with height above 3 m, and 618 plots had an interpreted VCC above 10 %. There were 141 plots with 100 % deciduous tree species, and 192 plots with 100 % coniferous tree species, thus the majority of sample plots had mixed tree species composition.

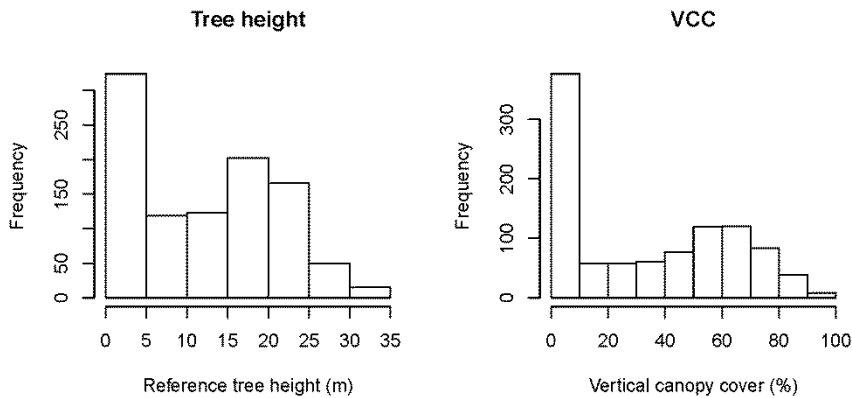


Figure 2. Histogram of interpreted tree height, and interpreted vertical canopy cover, in sample plots in Paper I.

In Paper II, visual stereo interpretation of land cover, dominating tree species, and diffuse canopy cover in the UltraCam Xpwa images was used to select the location of the 288 reference plots, which were circular with a radius of 20 m (Figure 1). The location of the reference plots was limited to the area covered by ALS data with a maximum scan angle of 10°. Vegetation ratio (VR) defined as the number of points above a height threshold (t) divided by the total number of points (Nilsson 1996), was used as reference data. VR was calculated per reference plot by using ALS point cloud data (see Section 3.2.1 for details) (Table 4).

Table 4. Statistics of reference plots used in Paper II. Height information and vegetation ratio (VR) was derived from ALS data.

Strata	Unmanaged	Deciduous	Wetland	Managed Forest
Number of reference plots	23	74	42	149
Range of h90 (m)	10 – 21	0 – 25	1 – 17	1 – 31
Mean of h90 (m)	15	16	8	15
SD of h90 (m)	3	5	4	7
Range of VR _{ALS} (%)	25 – 81	0 – 92	0 – 72	0 – 99
Mean VR _{ALS} (%)	58	33	30	53
SD of VR _{ALS} (%)	15	23	23	30
Dominant tree species	Scots Pine	Broadleaved trees, Birch	Scots Pine	Norway Spruce, Scots Pine, Birch

Abbreviations: h90 = height percentile 90. SD = standard deviation. VR_{ALS} = Vegetation ratio derived from ALS data.

3.2 Methods

3.2.1 Processing of ALS data

In Paper I, ALS data were classified as ground or non-ground returns using the method presented by Axelsson (1999) and a DEM with 0.5 m grid cell size was created by setting each cell value to the mean z-value of ground-classified laser returns within the cell. An interpolated value was assigned to raster cells without any ground-classified laser returns.

In Paper II, the ALS point cloud was classified as ground or non-ground returns using the method by Axelsson (1999, 2000). Flight line overlap was removed and the height of the laser returns was normalized to above ground (Isenburg 2015). First and single returns were kept and the point cloud was thinned down to one point per 0.5 m × 0.5 m grid cells, where one randomly selected point for each cell was kept. This was done in order to avoid effects of uneven point densities. The ALS point cloud was used to generate a DEM, as well as to calculate a reference vegetation ratio (VR_{ALS}) for each reference plot. Three different height thresholds (*t*) were tested, namely 1, 2, and 3 m above ground to produce three separate VR_{ALS_{*t*}}.

3.2.2 Image matching

In this thesis, the focus has been on using the photogrammetric software solutions from MATCH-T DSM by Inpho/Trimble, and SURE by nFrames. In Paper I, MATCH-T DSM version 5.2.1 was used by Lantmäteriet to produce three different DSMs: two by using the 4800 m images with two different along-track stereo overlaps (80% and 60%, respectively), a third DSM was

derived from the 1200 m images. MATCH-T DSM version 5.2.1 used a combination of feature-based matching (FBM) and least squares matching (LSM) to match homologous points in stereo models (Anon. 2009, Lemaire 2008).

In Paper II, two different image matching software solutions were applied to the same image set (Table 2) resulting in two different image-based point clouds, thus enabling a comparison. The first image matching software was MATCH-T DSM version 6.1 by Trimble, which used a combination of feature-based matching at low image pyramid levels and cost-based matching at the highest pyramid levels (Anon 2014a). The second image matching software was SURE version 1.1.1.3 by nFrames GmbH (Rothermel et al. 2012), which used an algorithm based on semi-global matching (SGM) by Hirschmüller (2008) (Rothermel et al. 2012). LAStools (Isenburg 2015) was used for further processing of the image-based point cloud datasets in Paper II; the height of each point cloud dataset was normalized to above ground, using the DEM from ALS data, and the point clouds were clipped to the reference plots. Vegetation ratio (VR_M) was calculated per plot. $t = 1, 2,$ and 3 m above ground, were used to produce three separate VR_M per image-based point cloud dataset.

3.2.3 Canopy Height Models

In Paper I, canopy height models (CHMs) were derived by normalizing the DSMs using the DEM derived from ALS data. The CHMs were manually checked for errors. A minor displacement in height between the DEM and the DSMs was detected over roads. This displacement was within the standard error inherent in block triangulation of the aerial images, which is approximately 0.8 m for a GSD of 0.5 m, and 0.35 m for a GSD of 0.25 m (Anon. 2013), and the observed errors were therefore considered acceptable. Water surfaces were given a null value. In addition to the original CHMs, modified versions were produced by resampling and median filtering. Nearest-neighbor resampling was used to produce CHMs with pixel sizes from 0.5 m; 1 m; 2 m; 3 m... up to 10 m. A median filter was expected to have a positive effect on the segmentation of vegetation patches. Median filters with kernel window sizes of 3×3 , 5×5 , 7×7 , 9×9 , and 11×11 pixels were applied to the original CHMs. The combination of resampling and filtering was also tested.

In Paper II, the normalized image-based point clouds were used to generate CHMs where the grid cells received the height value of the highest point within each cell, and cells wherein no points fell were set to zero height above ground. The CHMs were clipped to the reference plots and vegetation ratio (VR_{CHM}) was calculated per plot as the proportion of grid cells above $t = 3$ m, divided by

the total number of grid cells per plot. Grid cell sizes of 0.5; 0.75; 1; and 2 m were tested, resulting in four VR_{CHM} per matching method.

3.2.4 Segmentation (paper I)

Segmentation was done using the software eCognition 3.0 (Definiens Imaging GmbH Munich). The segmentation was performed on the CHM. The segmentations resulted in polygons representing so-called object primitives (Benz et al. 2004). Smoothing was applied to the segmentations to test whether the visual appearance of the segments could be improved without loss of accuracy.

3.2.5 Evaluation of segmentation (paper I)

Segmentations were visually inspected by considering the agreement of delineations to each corresponding CHM and to features in a CIR orthophoto. Standard deviation (SD) of tree height within segments was used as a measure of homogeneity within segments, with respect to canopy height, and calculated using the grid of sample plots.

3.2.6 Evaluation of tree height (paper I)

Linear regression was used to model the agreement between reference tree height and height percentiles extracted from the CHMs. Linear models were fitted on two levels: segment and sample plot level respectively, using the ordinary least squares method.

The dependent variable at segment level, mean reference tree height, was calculated as the sum of the reference tree heights of sample plots within each segment, divided by the number of sample plots within each segment. The predictor variable at segment level was calculated as height percentiles 70, 80, 90, 95, 96... 100 per segment from each original corresponding CHM.

The interpreted mean tree height per sample plot was used as dependent variable at the sample plot level regression analysis. Predictor variables were height percentiles 70, 80, 90, 95, 96... 100 calculated from the CHMs. At sample plot level, tests were made to exclude plots with vertical canopy cover below 10 %. Linear models were also fitted to plots with 100 % deciduous or coniferous tree species, respectively.

Leave-one-out cross-validation was used for accuracy estimation and the results were evaluated using root mean square error (RMSE). For each fitted model, the value of q was calculated, which is the square root of the ratio of the predicted sum of squares of the residuals to the ordinary sum of squares of the residuals, to test for over-fitting.

3.2.7 Estimation of vertical canopy cover (paper II)

Linear regression was applied per stratum, using the VR_{ALS_t} (vegetation ratio derived from ALS) as dependent variable and VR_{M_t} (vegetation ratio derived from image-based point cloud data) as independent variable. The regressions were set up based on t , meaning that $VR_{ALS_{t1}}$ was used for $VR_{M_{t1}}$, and so on. Leave-one-out cross-validation was used for accuracy estimation and the results were evaluated using root mean square error (RMSE) and relative RMSE (rRMSE) calculated as the RMSE divided by the mean vegetation ratio derived from ALS. For each fitted model, the value of q was calculated to test for over-fitting.

A similar setup was used to apply linear regression using the VR_{ALS3} as dependent variable and VR_{CHM} as independent variable.

4 Results and general discussion

4.1 General results

The most important results from the studies were:

- Segmentation using a CHM based on 3D information derived by image matching was successful in the sense that the produced segments had a relatively low SD of height above ground,
- The standard aerial images and stereo overlap available in Sweden is sufficient when aiming to produce segments corresponding to relatively large units, such as forest stands,
- Tree height in the CHM corresponded well with measurements via visual interpretation and tree height estimation using height percentiles from a CHM as predictor yields relatively high accuracy,
- Smoothing of the segments improved the visual impression of the segments without increasing the SD of vegetation height within the segments,
- Vertical canopy cover estimation using 3D information derived by image-matching as predictor shows promise in the interval of 15 – 85 % cover,
- The two different image matching software solutions yielded similar results.

Combining the results from papers I and II show that 3D information derived by image matching of the standard aerial images available in Sweden is potentially useful for mapping relatively large units such as forest stands, where the information is aggregated over an area.

4.2 Segmentation (paper I)

The segmentation of vegetation patches of homogeneous height, e.g. forest stands, was successful considering the visual impression of the segments in

relation to their corresponding CHM (Figure 3), a visual comparison to an orthophoto covering the study area, and the relatively low standard deviation (SD) of the reference tree height within the segments.

Resampling and filtering of the CHMs prior to segmentation resulted in slightly lower SD of tree height within segments, while smoothing made little difference (Table 5).

Table 5. Standard deviation of reference tree height within segments (m).

	CHM A	CHM B	CHM C
CHM used for segmentation	4800 m, 60/30 %	4800 m, 80/30%	1200 m, 80/60%
Original CHM	4.1	4.7	4.8
Resampled CHM	3.9 (1 m)	4.4 (2 m)	4.3 (2 m)
Filtered CHM	3.8 (5 × 5)	4.2 (11 × 11)	4.4 (9 × 9)
Resampled & Filtered CHM	3.7 (1 m, 3 × 3)	4.4 (2 m, 11 × 11)	4.3 (2 m, 5 × 5)

Abbreviations: CHM = canopy height model; 4800 m, 1200 m = flight altitude; 60/30, 80/30, 80/60 = stereo overlap (%); (1 m, 2 m) = pixel size after resampling; (5 × 5, 9 × 9, 11 × 11) = median filter kernel window size (pixels); First line represents results based on the original CHMs. The rest is a summary of the lowest standard deviation of tree height within segments based on the pre-processed CHMs (resampled, filtered, and combination of both resampling and filtering).

Elongated segments along forest edges were considered as erroneous since visual interpretation wouldn't result in such delineations due to limits such as minimum mapping unit and minimum width of a segment (Allard et al. 2003). There are several potential reasons for these segments being created;

- the actual tree height being lower along forest edges and thus reflected in the CHM,
- limited performance of image matching, such as the smoothing effect of area-based matching (St Onge et al. 2008),
- interpolation during conversion to grid,
- the segmentation method being set to allow the connection of areas of similar height by narrow sections, and
- occlusion or shadows, which causes mismatches, or no matches.

The DSMs used in paper I were derived directly in MATCH-T DSM, meaning that the image matching software used in paper I was not set to deliver image-based point clouds, thus there was no insight to the completeness of the image-based point clouds or to how the interpolation from point clouds to DSMs was done. The effect of interpolation from point cloud to grid could have been prevented by performing the interpolation using another, controlled solution.

Elimination of elongated segments could be done by shrink and expand operations (e.g. Waser et al. 2015). A similar approach would be to utilize the

GIS and search for narrow sections, cut these at the point where minimum width is exceeded and merge the narrow pieces to adjacent segments with similar height.

Adding spectral information could have improved the results of segmentation, especially if tree species could be separated. However, using of the spectral information in aerial images calls for radiometric correction (Korpela et al. 2011). An alternative source of spectral information is optical satellite data (e.g. Reese et al. 2015).

The potential effect of view angle (St Onge et al. 2015, Honkavaara et al. 2012) on the image matching products, such as a CHM, was not investigated in this thesis.

The CHM derived from standard aerial images available in Sweden lacked details such as small gaps within dense canopy, and single trees in open areas were occasionally missed (Figure 3a), while the CHM derived from images with a larger stereo overlap and higher spatial resolution showed more detail such as individual tree tops and small canopy gaps (Figure 3c), which is in line with observations by Hirschmugl (2008). However, the objective of Paper I was segmentation of large patches of vegetation with homogeneous height, which is why the methods for preprocessing, segmentation and evaluation were insensitive to details, or the lack thereof.

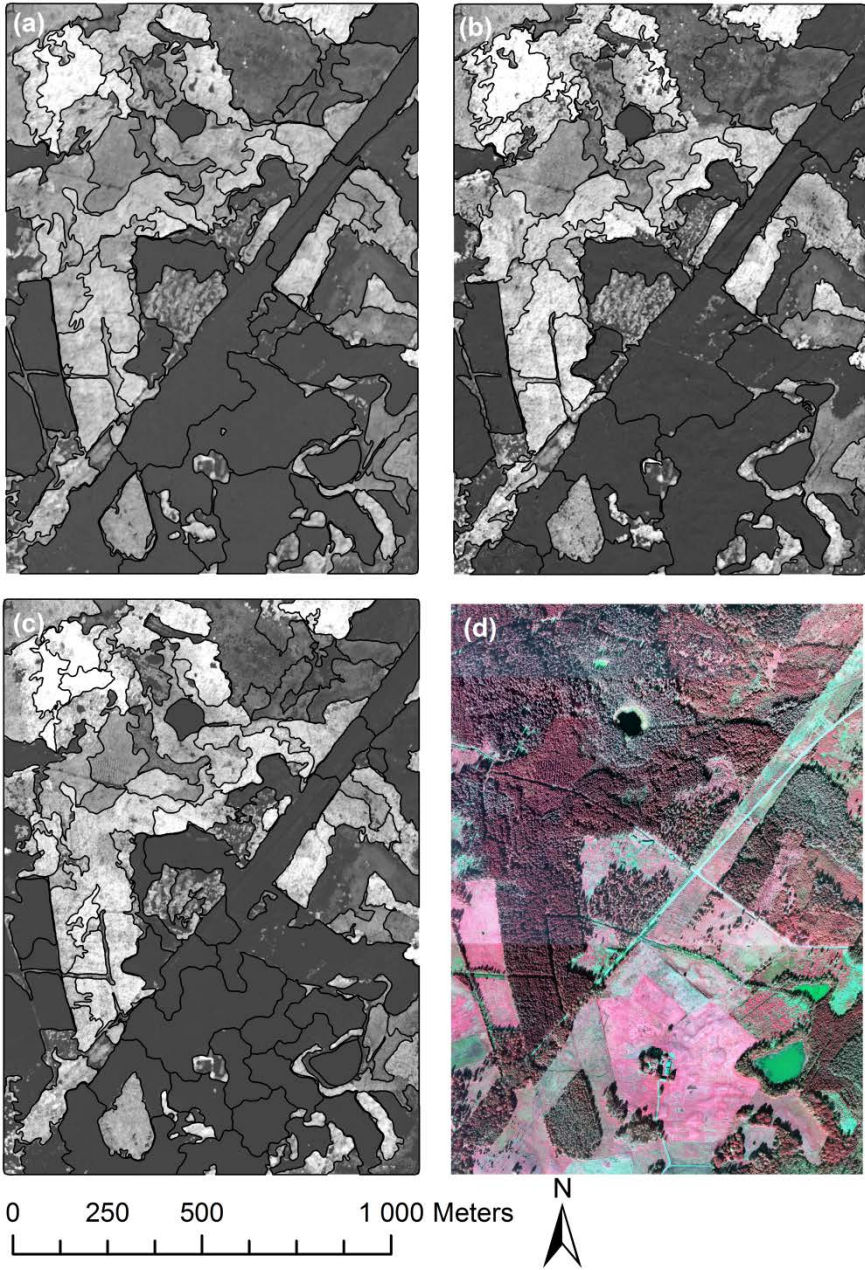


Figure 3. Canopy height models (CHM) with corresponding, smoothed segments. (a) CHM based on aerial images acquired at 4800 m above ground level (a.g.l.) and stereo overlap of 60 % along-track; (b) CHM based on aerial images acquired at 4800 m a.g.l. and stereo overlap of 80 % along-track; (c) CHM based on aerial images acquired at 1200 m a.g.l. and stereo overlap of 80 % along-track; (d) colour-infrared orthophoto of the study area derived from aerial images acquired at 1200 m a.g.l.

4.3 Tree height estimation (paper I)

Tree height estimations on the segment level resulted in relative root mean square error (rRMSE) of 15.1 – 18.3 % (Table 6). Corresponding results on sample plot level were at their best an rRMSE of 9.8 % for plots with 100 % coniferous tree species and canopy cover above 10 % (Table 7). The results by Bohlin et al. (2012) and Nurminen et al. (2013) were better, with accuracies at rRMSE 8.8 %, and 6.8 %, respectively. These higher accuracies were obtained using the image-based point cloud rather than a CHM, as was used in paper I. Thus, image-based point cloud data is potentially useful for mapping tree height.

Table 6. Results of tree height estimation at segment level.

.CHM	n	Post-processing	Y	X	RMSE (m)	rRMSE (%)
A	70		Tree height	h95	2.5	18.3
A	68	Smoothing	Tree height	h95	2.2	16.0
B	58		Tree height	h99	2.3	16.3
B	59	Smoothing	Tree height	h98	2.2	15.4
C	82		Tree height	h96	2.3	18.0
C	83	Smoothing	Tree height	h95	2.0	15.1

Abbreviations: CHM = canopy height model; n = number of segments; Y = dependent variable; X = independent variable. h95 = height percentile 95 extracted from CHM.

Table 7. Results of tree height estimation at sample plot level.

CHM	n	Subset	Y	X	RMSE (m)	rRMSE(%)
A	716		Tree height	h97	3.6	21.5
B	716		Tree height	h90	4.0	24.0
C	716		Tree height	h99	3.8	23.1
A	618	>10 % CC	Tree height	h90	2.7	15.6
A	192	Coniferous	Tree height	h98	2.5	12.1
A	179	Coniferous >10 % CC	Tree height	h97	2.1	9.8
A	141	Deciduous	Tree height	h98	4.5	30.1
A	87	Deciduous >10 % CC	Tree height	h98	2.6	16.2

Abbreviations: CHM = canopy height model; n = number of sample plots; Coniferous = 100% coniferous tree species; Deciduous = 100% deciduous tree species; Y = dependent variable; X = independent variable; h90 = height percentile 90 extracted from CHM.

High standard deviation (SD) of tree height was observed in segments with sparse canopy cover, and tree height estimation accuracy improved for models fitted to sample plots with vertical canopy cover above 10 % (compare Figure 4b and c, and Table 7). Thus, vertical canopy cover might influence the tree height estimation, which is in line with the findings of Waser et al. (2015) who

observed erroneous classification of forest or non-forest along forest edges and in areas with sparse tree cover. Considering this, it would be valuable to get accurate information on vertical canopy cover from image-based point clouds, or surface models.

St Onge et al. (2015) found that tree species had an influence of the accuracy of tree height estimation, thus classification of tree species could improve the accuracy. Similar observations were made in paper I, with lower accuracy of tree height estimation in a relatively small number of sample plots dominated by deciduous tree species (Figure 4e). A potential solution would be to utilize the spectral information available in the aerial images (e.g. Rahlf et al. 2015).

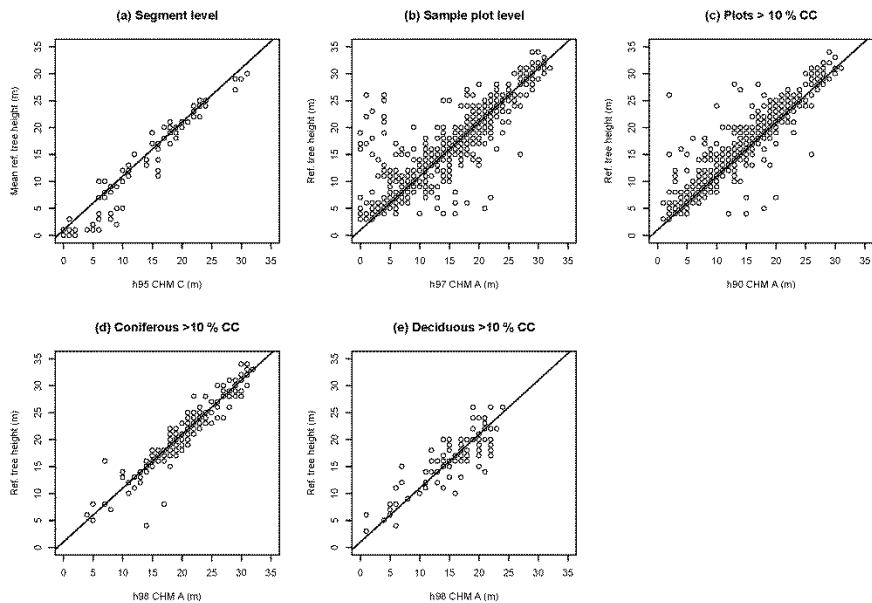


Figure 4. Interpreted tree height against height percentiles extracted from CHM with 1:1-line as reference. (a) Mean interpreted tree height per segment against percentile 95 from CHM C. (b) Interpreted tree height per sample plot against percentile 97 from CHM A. (c) Interpreted tree height in sample plots with canopy cover (CC) above 10 % against percentile 90 CHM A. (d) Interpreted tree height in sample plots with 100 % coniferous tree species and more than 10 % CC against percentile 98 from CHM A. (e) Interpreted tree height in sample plots with 100 % deciduous tree species and more than 10 % CC against percentile 98 from CHM A.

4.4 Vertical canopy cover (paper II)

Estimation of vertical canopy cover (VCC) using vegetation ratio derived from image-based point clouds (VR_M) calculated as the proportion of heights above

a height threshold resulted in models with poor fit. VCC was underestimated when canopy cover was sparse and overestimated when canopy cover was dense. The models were relatively linear between 15 % and 85 % canopy cover (Figure 5, Table 8). Using VR derived from CHMs (VR_{CHM}) wherein no data cells received zero height above ground yielded similar results (Figure 6, Table 8). Thus, this attempt to compensate for the lack of canopy gaps in areas with dense tree cover was not sufficient. However, the results were better than previously reported by Vastaranta et al. (2013) who found that VR calculated as the proportion of cells above 2 m height in a CHM, derived by image matching and normalized using ALS data, reached 100 % already at low basal area (10 – 20 m²/ha). Comparison to the results by Vastaranta et al. (2013) is most relevant for the Managed stratum, considering tree species composition and land use.

The overestimation of vertical canopy cover by using VR_M , and VR_{CHM} , was seemingly larger in the Managed stratum compared to the Deciduous stratum (Figure 5 and 6). However, this comparison is based on a low number of reference plots with VR_{ALS} above 80 % in the Deciduous stratum. Separating the reference plots into different strata improved the accuracy for the Deciduous stratum (Table 8), but further study is needed to answer whether the difference is related to land use, or tree species, or a combination of these factors. The observation that there is a difference related to tree species is nonetheless in line with the results in St Onge et al. (2015).

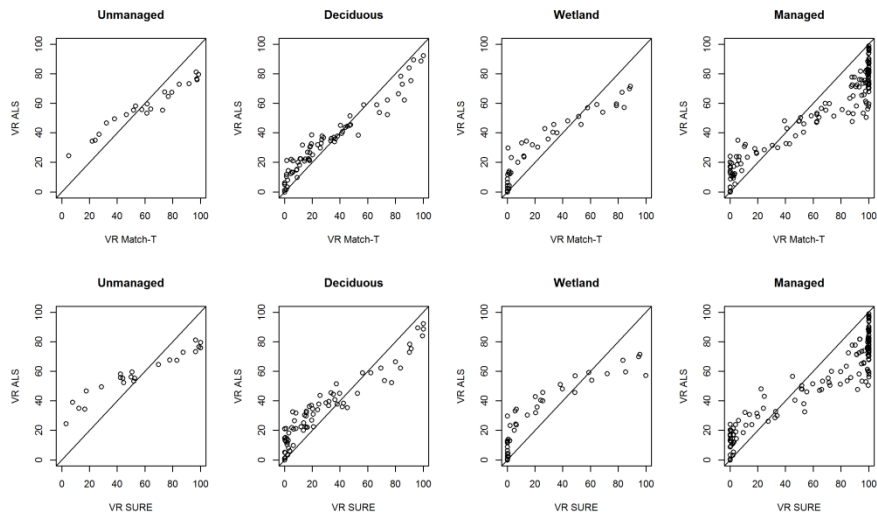


Figure 5. Vegetation ratio (VR) derived from ALS data (VR_{ALS}) per stratum against VR calculated from image-based point clouds (VR_M). Upper row is VR_{ALS} against VR_M from MATCH-T. Bottom row is VR_{ALS} against VR_M from SURE.

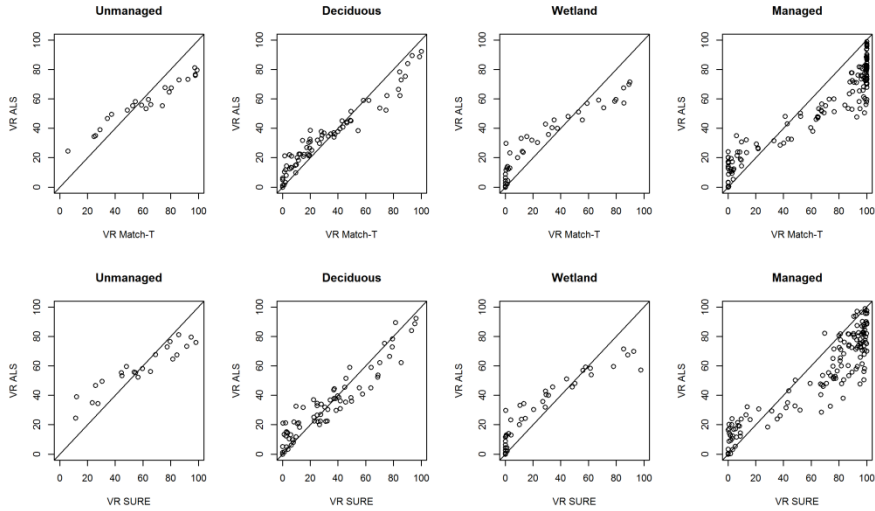


Figure 6. Vegetation ratio (VR) derived from ALS data (VR_{ALS}) per stratum against VR calculated from CHMs based on image-based point clouds (VR_{CHM}). Upper row is VR_{ALS} against VR_{CHM} from MATCH-T. Bottom row is VR_{ALS} against VR_{CHM} from SURE.

Table 8. Results of linear regression with VR_{ALS} as dependent variable (Y) and VR_M and VR_{CHM} , respectively, as independent variable (X). $t = 3$ m above ground. All coefficients were statistically significant with p -value > 0.001 for the t -test.

Y	X		Full	Stratum			
			dataset	Unmanaged	Deciduous	Wetland	Managed
			n = 288				
VR_{ALS}	VR_M	adj. R^2	0.91	0.95	0.93	0.87	0.90
		RMSE	8.4	3.5	6.0	8.3	9.5
	rRMSE	18.9	6.1	18.2	27.8	18.1	
VR_{ALS}	VR_M	adj. R^2	0.89	0.93	0.90	0.80	0.89
		RMSE	9.7	4.3	7.5	10.6	10.1
	rRMSE	21.6	7.3	22.4	35.5	19.2	
VR_{ALS}	VR_{CHM}	adj. R^2	0.91	0.95	0.94	0.88	0.90
		RMSE	8.5	3.6	5.9	8.1	9.8
	rRMSE	18.9	6.2	17.8	27.1	18.5	
VR_{ALS}	VR_{CHM}	adj. R^2	0.87	0.86	0.89	0.85	0.87
		RMSE	10.0	5.7	7.7	9.0	11.1
	rRMSE	22.4	9.9	23.1	30.2	21.1	

The use of a large reference plot size and the small canopy gap size in the Unmanaged stratum led to insufficient number of reference plots with low VR (Figure 5 and 6). The opposite situation was observed in the Wetland stratum

where the small tree crown size led to insufficient number of reference plots with high VR. Thus, a more appropriate sampling method should be used.

The findings in paper II are based on image matching of standard aerial images available in Sweden, meaning that the results might be influenced by the limitation to using aerial images with stereo overlap below recommendations (Anon 2014a, Anon 2014b). See Figure 7 and 8 for examples of point clouds from ALS and image-based point clouds derived using the two different image matching software.

As mentioned before, to improve the accuracy of canopy cover estimation there is a need for development of methods that are tailored to image-based point clouds. Previous studies have used methods developed for ALS point clouds (Vastaranta et al. 2013, Stepper et al. 2015a, White et al. 2015), though ALS and cameras are different sensors which leads to inherent differences in the point clouds (Baltsavias 1999, Figure 7 and 8). The introduction of a standard method for analysis of image-based point clouds could enable comparison of results over different regions, and in different canopy structure types. Considering the interest in using aerial images for generation of image-based point cloud data or surface models for vegetation mapping, new methods for analysis of such data are likely to emerge. Using a different method, such as tree detection or segmentation of vegetation with a height of 3 m above ground might result in more accurate estimation of vertical canopy cover. Perhaps the method used by Waser et al. (2015) is preferable, i.e. classification of pixels in a CHM based on a height threshold, provided that the erroneous classifications along forest edges and in sparsely covered areas can be avoided. An attempt to use aggregated height, i.e. the sum of height of detected trees within a plot, as a measure of canopy cover (Granholtm et al. 2015) has shown promise, but further development is needed.

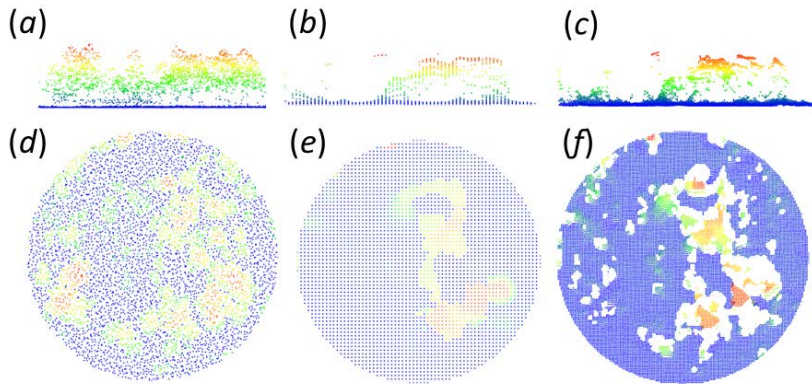


Figure 7. Normalized and height coloured point clouds covering a reference plot in the Wetland stratum with partial canopy cover of Scots pine. The vegetation ratio (VR) derived from ALS data = 35 % and height percentile 90 = 8 m. Upper row is in horizontal view and bottom row is viewed from atop. No data areas are white. (a) and (d) ALS point cloud; (b) and (e) MATCH-T; (c) and (f) SURE.

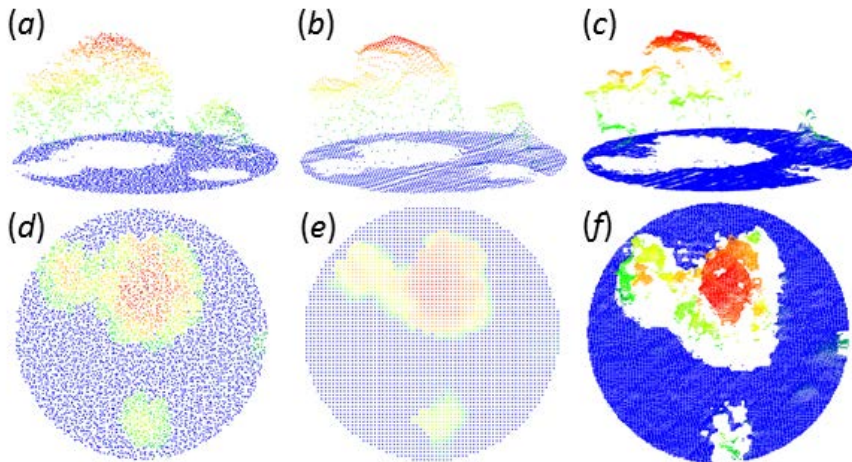


Figure 8. Normalized and height coloured point clouds covering a reference plot in the Deciduous stratum with partial canopy cover of broadleaved trees. The vegetation ratio (VR) derived from ALS data = 33 % and height percentile 90 = 16 m. Upper row is viewed from the side and bottom row is viewed from atop. No data areas are white. (a) and (d) ALS point cloud; (b) and (e) MATCH-T; (c) and (f) SURE.

5 Conclusions

We have only seen the beginning of using image-based point cloud data for vegetation mapping. This thesis covers merely a few details when it comes to exploring the utility of such data in segmentation based on vegetation height, and estimating canopy cover in common Swedish hemi-boreal vegetation types.

In this thesis, the focus has been on exploring the usefulness of image-based point cloud data, and surface models derived from them, in vegetation mapping. More specifically the segmentation of vegetation patches of homogeneous height, as well as quantification of vegetation within small patches, such as height above ground and cover.

Automatic segmentation based on a canopy height model (CHM) produced polygons wherein the vegetation height varied relatively little. The resulting delineations would need to be manually checked for accuracy, and manually edited. Further development is needed, for instance to include spectral information which would enable tree species classification and thereby improve segmentation results. There is potential in using surface models for automatic segmentation of areas with vegetation of homogeneous height above ground, which would reduce the need for manual delineation of forest areas.

The accuracy of tree height estimation was similar to slightly lower compared to previous studies, confirming that height information derived by image matching is of potential use for application in vegetation mapping.

The accuracy of vertical canopy cover estimation was in line with or slightly better compared to the general findings of previous studies conducted in coniferous dominated forests (Vastaranta et al. 2013, White et al. 2015). To my knowledge, there are no directly comparable results from studies conducted in hemi-boreal deciduous forests, nor in wooded pasture. The results show promise, as well as limitations of the used methods. The achieved accuracy of vertical canopy cover estimation using vegetation ratio wasn't satisfactory,

thus new methods for deriving vertical canopy cover from image-based point clouds and surface models are needed.

The aerial images used in the studies represent the regularly updated digital aerial imagery available in Sweden, showing the potential utility for vegetation mapping. The investigations have been limited to using products derived by the photogrammetric software available by department licence; MATCH-T DSM by Inpho/Trimble, and SURE by nFrames. There is a lack of image matching solutions which are optimal for matching images covering vegetated areas. Thus, the results presented in this thesis are limited to the used imagery, matching strategies, methods of evaluation, and the test area. However, the development of digital cameras as well as image matching software is ongoing, meaning that someday there will hopefully exist solutions specifically tailored to the needs of vegetation mapping. In a near future there will be image-point cloud data available for large areas of Sweden, among other jurisdictions with repeated acquisition of national coverage of stereo aerial imagery and an accurate and detailed digital elevation model.

References

- Allard, A., B. Nilsson, K. Pramborg, G. Ståhl, and S. Sundquist (2003). *Manual for Aerial Photo Interpretation in the National Inventory of Landscapes in Sweden, NILS*. Department of Forest Resource Management, Swedish University of Agricultural Sciences, Umeå.
- Andersson, L (2010). Geographical Vegetation Data of Lantmäteriet in Sweden. In *Mapping and Monitoring of Nordic Vegetation and Landscapes, Conference Proceedings. Viten fra Skog og landskap 01/10*, edited by A. Bryn, W. Dramstad, and W. Fjellstad, 9–12. Ås: Norsk institutt for skog og landskap.
- Anonymous (2009). *Match-TDSM 5.2 Reference Manual*. Stuttgart: INPHO GmbH.
- Anonymous (2013). *Produktbeskrivning: Digitala Flygbilder. Version 1.2. GSD Geografiska Sverigedata™*. Gävle: Lantmäteriet.
- Anonymous (2014a). Trimble. *Reference Manual of the software package Match-T DSM 6.0*. Inpho® software.
- Anonymous (2014b). nFrames. *SURE – Photogrammetric Surface Reconstruction from Imagery. Manual, version 12/5/14*.
- Axelsson, P (1999). Processing of Laser Scanner Data – Algorithms and Applications. *ISPRS Journal of Photogrammetry and Remote Sensing* 54 (2–3): 138–147. doi:10.1016/S0924-2716(99)00008-8.
- Axelsson, P (2000). DEM Generation from Laser Scanner Data Using Adaptive TIN Models. *International Archives of the Photogrammetry, Remote Sensing and Spatial Information Sciences XXXIII (B4/1)*: 110–117.
- Baatz, M., and A. Schäpe. (2000). Multiresolution Segmentation - An Optimization Approach for High Quality Multi-Scale Image Segmentation. In *Angewandte Geographische Informations-Verarbeitung XII*, edited by J. Strobl, T. Blaschke, and G. Griesebner, 12–23. Wichmann: Heidelberg.
http://www.ecognition.com/sites/default/files/405_baatz_fp_12.pdf
- Baltsavias, E. P. (1999). A Comparison between Photogrammetry and Laser Scanning. *ISPRS Journal of Photogrammetry and Remote Sensing* 54 (2–3): 83–94. doi:10.1016/S0924-2716(99)00014-3.

- Baltsavias, E. P., A. Gruen, H. Eisenbeiss, L. Zhang, and L. Waser. (2008) High-Quality Image Matching and Automated Generation of 3D Tree Models. *International Journal of Remote Sensing* 29: 1243–1259. doi:10.1080/01431160701736513.
- Benz, U., P. Hofmann, G. Willhauck, I. Lingenfelder, and M. Heynen. (2004). Multi-Resolution, Object-Oriented Fuzzy Analysis of Remote Sensing Data for GIS-Ready Information. *ISPRS Journal of Photogrammetry and Remote Sensing* 58: 239–258. doi:10.1016/j.isprsjprs.2003.10.002.
- Blaschke, T. (2010) Object based image analysis for remote sensing. *ISPRS Journal of Photogrammetry and Remote Sensing*, 65 (1): 2-16
- Boberg, A (2001). *Introduktion till fotogrammetrin*. Kungliga tekniska högskolan. Stockholm.
- Bohlin, J., J. Wallerman, and J. E. S. Fransson. (2012). Forest Variable Estimation Using Photogrammetric Matching of Digital Aerial Images in Combination with a High-Resolution DEM. *Scandinavian Journal of Forest Research* 27: 692–699. doi:10.1080/02827581.2012.686625.
- Boresjö-Bronge, L., and B. Näslund-Landenmark. (2002). Wetland Classification for Swedish CORINE Land Cover Adopting a Semi-Automatic Interactive Approach. *Canadian Journal of Remote Sensing* 28: 139–155. doi:10.5589/m02-011.
- Cramer, M. and Haala, N. (2010) DGPF Project: Evaluation of Digital Photogrammetric Aerial-based Imaging Systems - Overview and Results from the Pilot Center. *Photogrammetric Engineering and Remote Sensing* 76 (9): 1019-1029
- FAO. (2010). Global Forest Resource Assessment 2010 Main Report. *FAO Forestry Paper 163*. Rome: Food and Agriculture Organization of the United Nations. <http://www.fao.org/docrep/013/i1757e/i1757e.pdf>
- Gao, T., Hedblom, M., Emilsson, T., Nielsen, A.B. (2014) The role of forest stand structure as biodiversity indicator. *Forest Ecology and Management* 330: 82–93
- Gardfjell, H. & Hagner, Å. (2011). *Instruktioner för Habitatinventering i NILS och MOTH, 2011*. Department of Forest Resource Management, Swedish University of Agricultural Sciences.Umeå.
- Ginzler, C. and Hobi, M. L. (2015) Countrywide Stereo-Image Matching for Updating Digital Surface Models in the Framework of the Swiss National Forest Inventory. *Remote Sensing* 7 (4): 4343-4370
- Gobakken, T., O. M. Bollandsås, and E. Næsset. (2015). Comparing Biophysical Forest Characteristics Estimated from Photogrammetric Matching of Aerial Images and Airborne Laser Scanning Data. *Scandinavian Journal of Forest Research* 30 (1): 73-86. doi:10.1080/02827581.2014.961954
- Granhölm, A., N. Lindgren, K. Olofsson, A. Allard and H. Olsson. (2015) Estimating vertical canopy cover using dense point cloud data from matching of aerial photos. In: *Proceedings of the 35th EARSeL Symposium – European Remote Sensing: Progress, Challenges and Opportunities* Stockholm, Sweden, June 15-18, 2015.
- Gunnarsson, U. and Löfroth, M. (2009). *Våtmarksinventeringen – resultat från 25 års inventeringar. Nationell slutrapport för våtmarksinventeringen (VMI) i Sverige. Rapport 5925*. Naturvårdsverket. Bromma, Sweden. Available from

- <https://www.naturvardsverket.se/Documents/publikationer/978-91-620-5925-5.pdf> [2015-11-17]
- Haala, N. (2014). *Dense Matching Final Report. EuroSDR, European Spatial Data Research, Official Publication No 64*. April 2014. Buchdruckerei Ernst Becvar, Vienna, Austria. Available from http://www.eurosd.net/sites/default/files/uploaded_files/eurosd_r_no64_c.pdf [2015-11-27]
- Haala, N. (2009). Comeback of digital image matching. *Photogrammetric Week '09*. Dieter Fritsch (Ed.) Wichmann Verlag, Heidelberg, 2009
- Haala, N. and Rothermel, M., (2012). Dense Multi-Stereo Matching for High Quality Digital Elevation Models. *PFG Photogrammetrie, Fernerkundung, Geoinformation*. Jahrgang 2012 (4): 331-343.
- Hagner, O., and H. Reese. (2007). A Method for Calibrated Maximum Likelihood Classification of Forest Types. *Remote Sensing of Environment* 110: 438–444. doi:10.1016/j.rse.2006.08.017.
- Hedblom, M., Söderström, B. (2011). Effects of urban matrix on reproductive performance of Great Tit (*Parus Major*) in urban woodlands. *Urban ecosystems* 15 (1): 167-180
- Heiskanen, J., B. Nilsson, A. Mäki, A. Allard, J. Moen, S. Holm, S. Sundquist and H. Olsson. (2008) *Aerial photo interpretation for change detection of treeline ecotones in the Swedish mountains. Arbetsrapport 242*. SLU, Umeå
- Hellesen, T. and L. Matikainen (2013). An object-based approach for mapping shrub and tree cover on grassland habitats by use of LiDAR and CIR orthoimages. *Remote Sensing* 5: 558 – 583.
- Heuchel, T., Köstli, A., Lemaire, C. and Wild, D. (2011) Towards a next level of quality DSM/DTM extraction with MATCH-T. *Photogrammetric Week '11* Dieter Fritsch (Ed.) Wichmann/VDE Verlag, Belin & Offenbach, 2011
- Hirschmugl, M. (2008). *Derivation of Forest Parameters from UltracamD Data*. PhD diss., Graz University of Technology.
- Hirschmüller, H. (2008) Stereo Processing by Semi-Global Matching and Mutual Information, *IEEE Transactions on Pattern Analysis and Machine Intelligence* 30(2): 328-341.
- Honkavaara, E., Ahokas, E., Hyypä, J., Jaakkola, J., Kaartinen, H., Kuittinen, R., Markelin, L., and Nurminen, K. (2006) Geometric test field calibration of digital photogrammetric sensors. *ISPRS Journal of Photogrammetry and Remote Sensing* 60 (6): 387-399.
- Honkavaara, E., Markelin, L., Rosnell, T. and Nurminen, K. (2012) Influence of solar elevation in radiometric and geometric performance of multispectral photogrammetry. *ISPRS Journal of Photogrammetry and Remote Sensing* 67: 13-26
- Honkavaara, E., Litkey, P., Nurminen, K. (2013) Automatic Storm Damage Detection in Forests Using High-Altitude Photogrammetric Imagery. *Remote Sensing* 5(3): 1405-1424
- Ihse, M. (2007). Color Infrared Aerial Photography as a Tool for Vegetation Mapping and Change Detection in Environmental Studies of Nordic Ecosystems: A Review. *Norwegian Journal of Geography* 61: 170–191. doi:10.1080/00291950701709317.
- Isenburg, M. (2015) *LAStools - efficient tools for LiDAR processing. Version 150526*, <http://lastools.org>.

- Jeglum, J., Sandring, S., Christensen, P., Glimskär, A., Allard, A., Nilsson, L. & Svensson, J. (2011). Main ecosystem characteristics and distribution of wetlands in boreal and alpine landscapes in Northern Sweden under climate change. In: *Grillo & Venora (Ed.), Ecosystems Biodiversity*, pages 193-218. Intech.
- Jennings, S. B., N. D. Brown, and D. Sheil. (1999). Assessing Forest Canopies and Understorey Illumination: Canopy Closure, Canopy Cover and Other Measures. *Forestry* 72: 59–74. doi:10.1093/forestry/72.1.59.
- Järnstedt, J., A. Pekkarinen, S. Tuominen, C. Ginzler, M. Holopainen, and R. Viitala. (2012). Forest Variable Estimation using a High-Resolution Digital Surface Model. *ISPRS Journal of Photogrammetry and Remote Sensing* 74: 78–84. doi:10.1016/j.isprsjprs.2012.08.006.
- Korpela, I. Heikkinen, V. Honkavaara, E. Rohrbach, F. and Tokola, T. (2011) Variation and directional anisotropy of reflectance at the crown scale - Implications for tree species classification in digital aerial images. *Remote Sensing of Environment* 115(8): 2062-2074
- Klang D. (2015) *Förstudie - Produktion av ytmodeller med hjälp av bildmatchning*. GeoXD AB. 2015-11-03. Stockholm.
- Leckie, D. G. Gougeon, F. A. Walsworth, N. and Paradine, D. (2003) Stand delineation and composition estimation using semi-automated individual tree crown analysis. *Remote Sensing of Environment* 85 (3): 355-369
- Leberl, F. Irschara, A. Pock, T. Meixner, P. Gruber, M. Scholz, S. and Wiechert, A. (2010) Point Clouds: Lidar versus 3D Vision. *Photogrammetric Engineering and Remote Sensing* 76 (10): 1123-1134
- Lemaire, C. 2008. Aspects of the DSM Production with High Resolution Images. *Proceedings of the ISPRS Congress, 3–11 July, Commission IV, WG IV/9, Beijing, China International Archives of the Photogrammetry, Remote Sensing and Spatial Information Sciences XXXVII (B4): 1143–1146*. http://www.isprs.org/proceedings/XXXVII/congress/4_pdf/200.pdf
- Lillesand, T.M., Keifer R.W. & Chipman J.W. (2008). *Remote Sensing and Image Interpretation*. 6th ed: John Wiley and Sons, Inc.
- Lim, K. Hopkinson, C. Treitz, P. (2008) Examining the effects of sampling point densities on laser canopy height and density metrics. *Forestry Chronicle* 84(6): 876-885
- Lindgren, N., P. Christensen, B. Nilsson, M. Åkerholm, A. Allard, H. Reese, and H. Olsson. (2015). Using Optical Satellite Data and Airborne Lidar Data for a Nationwide Sampling Survey. *Remote Sensing* 7: 4253-4267. doi:10.3390/rs70404253
- Matikainen, L. and K. Karila (2011) Segment-Based Land Cover Mapping of a Suburban Area - Comparison of High-Resolution Remotely Sensed Datasets Using Classification Trees and Test Field Points. *Remote Sensing* 3: 1777-1804
- McGlone, J.C. and Lee, G.Y.G. (2013) *Manual of Photogrammetry*. 6th ed. American Society for Photogrammetry and Remote Sensing.
- Middlebury Stereo Benchmark (2016) <http://vision.middlebury.edu/stereo/> [2016-03-16]
- Naturvårdsverket (2004). *Kartering av skyddade områden - Kontinuerlig naturtypskartering, Rapport 5391*. December 2004, Naturvårdsverket.
- Naturvårdsverket (2009). *Basinventering av Natura 2000 och skyddade områden 2004–2008 Beskrivning av genomfört projekt rapport 5990* • september 2009

- Naturvårdsverket. (2014) *Svenska Marktäckedata – Produktbeskrivning. Utgåva 1.2*, 2014-06-27. 48 pages. In Swedish only. Available from http://gpt.vic-metria.nu/data/land/SMD_produktbeskrivning_20140627.pdf [2015-11-17]
- Nilsson, M. (1996) Estimation of tree heights and stand volume using an airborne lidar system. *Remote Sensing of Environment* 56 (1): 1-7.
- Nilsson, M., K. Nordkvist, J. Jonzén, N. Lindgren, P. Axensten, J. Wallerman, M. Egberth, S. Larsson, L. Nilsson, J. Eriksson and H. Olsson. (Submitted) A nationwide forest attribute map of Sweden derived using airborne laser scanning data and field data from the national forest inventory.
- Nordkvist, K., Granholm, A., Holmgren, J., Olsson, H., and Nilsson, M. (2012). Combining optical satellite data and airborne laser scanner data for vegetation classification. *Remote Sensing Letters*. 3:5, 393-401
- Nurminen, K., M. Karjalainen, X. Yu, J. Hyypä, and E. Honkavaara. (2013) Performance of Dense Digital Surface Models based on Image Matching in the Estimation of Plot-Level Forest Variables. *ISPRS Journal of Photogrammetry and Remote Sensing* 83: 104–115. doi:10.1016/j.isprsjprs.2013.06.005.
- Nystrom, M. Lindgren, N. Wallerman, J. Grafstrom, A. Muszta, A. Nystrom, K. Bohlin, J. Willen, E. Fransson, J. E. S. Ehlers, S. Olsson, H. and Stahl, G. (2015) Data Assimilation in Forest Inventory: First Empirical Results. *Forestry* 6(12): 4540-4557
- Ottvall, R., Green, M., Lindström, A., Svensson, S., Esseen, P.-A. and Marklund, L. (2008) Distribution and habitat choice of the ortolan bunting *Emberiza hortulana* in Sweden. *Ornis Svecica* 18(1): 3-16.
- Ortega, M., Metzger, M.J., Bunce, R.G.H. Wrбка, T., Allard, A., Jongman, R.H.G. and Elena-Rosselló R. (2011): The potential for integration of environmental data from regional stratifications into a European monitoring framework. *Journal of Environmental Planning and Management*: 1-19 DOI:10.1080/09640568.2011.575698
- Pitt, D. G. Woods, M. and Penner, M. (2014) A Comparison of Point Clouds Derived from Stereo Imagery and Airborne Laser Scanning for the Area-Based Estimation of Forest Inventory Attributes in Boreal Ontario. *Canadian Journal of Remote Sensing* 40(3): 214-232
- Pekkarinen, A. (2002) A method for the segmentation of very high spatial resolution images of forested landscapes. *International Journal of Remote Sensing* 23(14): 2817-2836
- Rahlf, J. Breidenbach, J. Solberg, S. and Astrup, R. (2015) Forest Parameter Prediction Using an Image-Based Point Cloud: A Comparison of Semi-ITC with ABA. *Forests* 6(11): 4059-4071
- Rapinel, S., L. Hubert-Moy and B. Clément. (2015) Combined use of LiDAR data and multispectral earth observation imagery for wetland habitat mapping. *International journal of applied earth observation and geoinformation* 37: 56 – 64.
- Reese, H., Nilsson, M., Pahlen, T.G., Hagner, O., Joyce, S., Tingelöf, U., Egberth, M. and Olsson, H. (2003). Countrywide estimates of forest variables using satellite data and field data from the national forest inventory. *Ambio* 32(8): 542-548.
- Reese, H., Nyström, M., Nordkvist, K. and Olsson, H. (2014) Combining airborne laser scanning data and optical satellite data for classification of alpine vegetation. *International Journal of Applied Earth Observation and Geoinformation* 27: 81-90. Doi: 10.1016/j.jag.2013.05.003

- Reese, H., Nordkvist, K., Nyström, M., Bohlin, J. and Olsson, H. (2015) Combining point clouds from image matching with SPOT 5 multispectral data for mountain vegetation classification. *International Journal of Remote Sensing* 36 (2): 403 – 416. DOI: 10.1080/2150704X.2014.999382
- Remondino, R., Spera M.G., Nocerino, E., Menna, F. and Nex, F. (2014) State of the art in high density image matching. *The Photogrammetric Record* 29(146): 144–166 DOI: 10.1111/phor.12063
- Rothermel, M., K. Wenzel, D. Fritsch, and N. Haala. (2012). “SURE: Photogrammetric Surface Reconstruction from Imagery”. *Proceedings LC3D Workshop, December 2012*, Berlin, Germany, 9 pages.
- Skogsstyrelsen (2015). Skogliga grunddata. Available from <http://www.skogsstyrelsen.se/skogligagrunddata> [2016-03-16]
- SLU, 2015. *SLU Forest Map*, Dept. of Forest Resource Management, Swedish University of Agricultural Sciences. Available from <http://www.slu.se/sv/centrumbildningar-och-projekt/riksskogstaxeringen/tjanster-och-produkter/interaktiva-tjanster/slu-skogskarta/> [2015-11-27]
- Stepper, C., Straub, C. and Pretzsch, H. (2015a) Using semi-global matching point clouds to estimate growing stock at the plot level and stand levels: application for a broadleaf-dominated forest in central Europe. *Canadian Journal of Forest Research* 45: 111-123.
- Stepper, C. Straub, C. and Pretzsch, H. (2015b) Assessing height changes in a highly structured forest using regularly acquired aerial image data. *Forestry* 88(3): 304-316
- St-Onge, B., C. Vega, R. A. Fournier, and Y. Hu. (2008) Mapping Canopy Height Using a Combination of Digital Stereo-Photogrammetry and LiDAR. *International Journal of Remote Sensing* 29: 3343–3364. doi:10.1080/01431160701469040.
- St-Onge, B., Audet, F-A. and Begin, J. (2015) Characterizing the Height Structure and Composition of a Boreal Forest Using an Individual Tree Crown Approach Applied to Photogrammetric Point Clouds. *Forests* 6(11): 3899-3922
- Straub, C., Stepper, C., Seitz, R. and Waser, L. T. (2013) Potential of UltraCamX stereo images for estimating timber volume and basal area at the plot level in mixed European forests. *Canadian Journal of Forest Research-Revue Canadienne De Recherche Forestiere* 43(8): 731-741
- Ståhl, G., A. Allard, P.-A. Esseen, A. Glimskär, A. Ringvall, J. Svensson, S. Sundquist, P. Christensen, Å. Gallegos Torell, M. Högström, K. Lagerqvist, L. Marklund, B. Nilsson, and O. Inghe. (2011) National Inventory of Landscapes in Sweden (NILS) - Scope, Design, and Experiences from Establishing a Multiscale Biodiversity Monitoring System. *Environmental Monitoring and Assessment* 173: 579–595. doi:10.1007/s10661-010-1406-7.
- Vastaranta, M., M. A. Wulder, J. C. White, A. Pekkarinen, S. Tuominen, C. Ginzler, V. Kankare, M. Holopainen, J. Hyypä, and H. Hyypä. (2013) Airborne Laser Scanning and Digital Stereo Imagery Measures of Forest Structure: Comparative Results and Implications to Forest Mapping and Inventory Update. *Canadian Journal of Remote Sensing* 39: 382–395. doi:10.5589/m13-046.
- Vastaranta, M. Niemi, M. Wulder, M. A. White, J. C. Nurminen, K. Litkey, P. Honkavaara, E. Holopainen, M. and Hyypä, J. (2016) Forest stand age classification using time series of

- photogrammetrically derived digital surface models. *Scandinavian Journal of Forest Research* 31(2): 194 – 205.
- Wang, Z., C. Ginzler, and L. Waser. (2015). A Novel Method to Assess Short-Term Forest Changes Based on Digital Surface Models from Image-Based Point Clouds. *Forestry* 0: 1-12. doi: 10.1093/forestry/cpv012
- Waser, L., E. P. Baltasvias, K. Ecker, H. Eisenbeiss, E. Feldmeyer-Christe, C. Ginzler, M. Küchler, and L. Zhang. (2008). Assessing Changes of Forest Area and Shrub Encroachment in a Mire Ecosystem Using Digital Surface Models and CIR Aerial Images. *Remote Sensing of Environment* 112: 1956–1968. doi:10.1016/j.rse.2007.09.015.
- Wallerman, J. Bohlin, J. and Fransson, J. E. S. (2012) Forest height estimation using semi-individual tree detection in multi-spectral 3D aerial DMC data. In: *2012 IEEE International Geoscience and Remote Sensing Symposium*. Pages 6372-6375
- White, J. C., M. A. Wulder, M. Vastaranta, N. C. Coops, D. Pitt, and M. Woods. (2013). The Utility of Image-Based Point Clouds for Forest Inventory: A Comparison with Airborne Laser Scanning. *Forests* 4: 518–536. doi:10.3390/f4030518.
- White, J. C., Stepper, C., Tompalski, P., Coops, N. C. and Wulder, M. A. (2015) Comparing ALS and Image-Based Point Cloud Metrics and Modelled Forest Inventory Attributes in a Complex Coastal Forest Environment. *Forests* 6(10): 3704-3732.

Acknowledgements

Jag vill tacka min handledare Håkan Olsson, och mina biträdande handledare Anna Allard och Mats Nilsson, som anförtrodde mig uppdraget som doktorand inom EMMA-programmets WP3, och som stöttat mig genom goda råd och diskussioner.

Tack till Mikael Johansson på Lantmäteriet som införskaffade och tillhandahöll flygbilder till första studien. Tack Anders Ekholm för besöket på bildenheten, Lantmäteriet, samt Christer Sandberg för orientering av flygbilder och Bertil Hedquist för matchning av nämnda flygbilder.

Tack till min finansiär Naturvårdsverket, och mer specifikt Ola Inghe som skötte EMMA-programmet. Tack alla som arbetade inom EMMA-programmet för inspirerande samtal, speciellt Helle Skånes på Stockholms Universitet.

Tack alla på avdelningen för skoglig fjärranalys för er vänlighet. Tack för hjälp med fältutrustning och för att ni delar med er så generöst av er tid, kunskap och kod, samt nycklar när jag glömt dem hemma (speciellt Jonas Jonzén och Inka Bohlin). Tack Heather Reese för hjälp med språk, goda råd och ditt fantastiska lugn. Tack Nils Lindgren för praktisk hjälp med bearbetning av laserdata och medförfattandeskap på paper II. Tack till Johan Holmgren och Mattias Nyström för hjälp med laserdata. Tack Kenneth Olofsson för hjälp med bildanalys. Tack Eva Lindberg för hjälp under fältarbetet på Remningstorp, samt för sällskapet i stugan och på vår rundtur i regionen. Tack Johan Fransson för information om fältinventeringarna på Remningstorp, samt för att du roddar institutionen. Tack Michael Egberth för att du tar hand om våra ovärderliga data. Tack Karin Nordkvist för sällskap och hjälp under fältarbetet i trakterna kring Ockelbo, tänk om jag anat att jag skulle hitta en vän medan vi letade provytor i skogen. Tack Peder Axensten för hjälp att processa stora dataset. Tack Jörgen Wallerman för hjälp med R-script. Tack Mats Högström för hjälp att lösa GIS-problem. Tack Mona Forsman för svar på frågor om fotogrammetri och bildmatching, samt för att du lyssnar och

peppar. Tack Jonas Bohlin för tips och hjälp rörande bildmatchning. Tack Emma Sandström för hjälp att se det ljusa i tillvaron. Tack Henrik Persson för introduktionen till matchning med RSG, snart måste jag hinna testa det! Tack till arbetskamrater som passerat under åren; Andreas Pantze, Janne Heiskanen, Michael Gilichinsky, Jari Vauhkonen, och Alessandro Montagni. Ett postumt tack till Nelson Scherman för intressanta samtal över lunch och fika.

Tack alla på avdelningen för Landskapsanalys för praktisk hjälp med lån av tolkningsutrustning, samt beställning av flygbilder. Tack Marianne Åkerholm för flygbildstolkning inom vegetationsklassningsprojektet. Tack Anna Allard, Maud Tyboni och Björn Nilsson för undervisning i flygbildstolkning. Tack Sofia Jonsson, Eric Cronvall, Karin Pramborg, Karin Wikström, och Åsa Gallegos-Torell för trevliga stunder i NILS/Natura-tolkarrummen.

Tack Anne-Maj Jonsson, Carina Westerlund och Ylva Jonsson på administrativa enheten på SRH för att ni alltid vet hur man löser alla möjliga och omöjliga problem.

Jag vill tacka min familj för all uppmuntran längs vägen. Alice och Kalle, mina underbara barn, tack för alla hejarop! Daniel, min klippa. Tack för att du stöttar mig och bär upp vår tillvaro. Snart är jag klar och kan komma tillbaka.